FACULTY OF SCIENCE AND TECHNOLOGY

BACHELOR THESIS

Study programme / specialisation:

Bachelor in physics and mathematics

The spring semester, 20.22.

Open / Confidential

Stine Norli

.....

(signature author)

Author: Stine Aunøien Norli

Course coordinator: Alex Bentley Nielsen

Supervisor(s): Helena Kolesova

Thesis title: Weakly interacting dark matter miracle

Credits (ECTS): 20

Keywords:

The early Universe
Expansion
Standard Model
DarkSUSY
Thermal freeze out
WIMP miracle
Thermal and non thermal relics
Search for dark matter

Pages: 31

+ appendix: none

Stavanger, May 15th. 2022

date/year

Approved by the Dean 30 Sep 21
Faculty of Science and Technology

Acknowledgements

I would like to thank my supervisor Helena Kolesova, Postdoc at University of Stavanger, for excellent guidance throughout the semester. She was always interested in helping and was available whenever I needed help. I am grateful for all the time she has used to guide me and for all the new things I have learned from her. Thanks to Helena, I have really enjoyed this semester writing my thesis, and gotten the possibility to dive into the mystery of dark matter.

I would also like to thank Liva Sandvin Vangen, fellow student, for great discussions and motivation in understanding while writing our different thesis's.

Abstract

Dark matter is currently actively searched for in particle physics. In this thesis the weakly interacting massive particles (WIMPs) are looked at as possible dark matter candidates. The thesis focus on the mechanism called thermal freeze out and looks for approximate and numerical solutions related to the WIMP miracle. The Boltzmann equation is solved both by approximate solutions analytically, and by numerical solutions obtained from full calculations done in DarkSUSY. Information about the early Universe, the Standard Model, and evidence for dark matter is given as background for the thesis. The thesis will also include some discussion about searches for dark matter and other possible dark matter relics.

Contents

1 Introduction

Currently there are many particle physics experiments running in the search to detect dark matter particles. However, it is not easy to detect these particles. The main problem for detecting dark matter is that their assumed properties make it difficult. The reason that the particles are difficult to detect is that in particle physics, the dark matter particles are expected to be electrically neutral, uncoloured, weakly interacting and stable. Such particles cannot be found in the Standard Model, so we have to look beyond this model.
In this thesis the WIMP miracle is looked at. The WIMP miracle describes particles that go beyond the Standard Model. The particles extend from the Standard Model by supersymmetry (SUSY), and are thought to be weakly interacting and massive.
One of the most important things in observing dark matter is to measure the cosmological density of dark matter, which in my thesis is called the relic abundance. The relic abundance measures the amount of relics remaining from the early Universe, where the particles were produced. We get to the equation of the relic abundance by deriving the Boltzmann equation in Section 4.1. The Boltzmann equation is solved both analytically by approximate solutions, and numerically by the use of full calculations in DarkSUSY. With these results, a value for the dark matter interactions with the Standard Model particles is derived, and the relic abundance is derived. The different results from the Boltzmann equation are compared, and the interaction is also compared to the interactions in the Standard Model. The cross sections for weak interactions are found to be quite similar to the ones obtained for WIMPs.
In this thesis is first presented some necessary background material in Section 2. This section includes some useful conventions used throughout the thesis, the early Universe and its expansion, the Standard Model and some information for the DarkSUSY program used in the thesis. Section 3 contains the evidence for dark matter, while in Section 4 is presented the main topic for the thesis, the thermal freeze out mechanism. Results are included here, in Section 4. In the last section, Section 5, is included some experiments in the search for dark matter particles and some other possible dark matter relics. Conclusions are found in Section 6.

2 Background

2.1 Conventions

Throughout this thesis natural units with $c = \hbar = k_b = 1$ are used. With these assumptions in particle physics, temperatures and mass will be measured in units of energy, GeV.
$M_{\rm Pl} = 2.4 \times 10^{18}$GeV. In section 2.2 is defined the FLRW metric where the boldface, $\mathbf{x}^2$, means three-dimensional vector-form.

2.2 The early Universe

Section 2.2 and 2.2.1 are mostly based on [1] and [2]. The beginning of history of the Universe is set at t= 0. The scale factor $a(t)$ measures the relative expansion of the Universe and increase as a function of time.
The standard cosmological scenario is based on the FLRW model (Friedmann-Lemaitre-Robertson-Walker) [3]. This model assumes homogeneity and isotropy throughout the Universe, and it is a model on the space-time metric,

$$ds^2 = dt^2 - a^2(t)d\boldsymbol{x}^2 \tag{1}$$

where $d\mathbf{x}^2$ is in three dimensions and coordinate $\mathbf{x}$ is comoving. Observationally, the space is taken to be Euclidean, so it is flat.
Currently the total energy density in the Universe is dominated by the cosmological constant, Λ. In the recent past, matter was dominating, and at the beginning of the Universe radiation was dominating. The scale factor $a(t)$ for the radiation dominated era is $a(t) \propto t^{1/2}$. For the matter dominated era the scale factor depends on the relative values of Ω_m and Ω_Λ, but for the simplest case it is taken to be $a(t) \propto t^{2/3}$. For the era where the cosmological constant dominates over matter, the scale factor $a(t)$ is assumed to increase exponentially. The temperature varies for all the eras since $T \propto a^{-1}$ [4].
We can relate the Hubble parameter to the scale factor $a(t)$ by the first equality below in Eq.(2). This relation is related again to the radiation dominated Universe where freeze out is assumed to happen [5].

$$H^2 = \left(\frac{\frac{da}{dt}}{a}\right)^2 = \left(\frac{1}{2t}\right)^2 = g_* \frac{\pi^2}{90}\frac{1}{M_{Pl}^2}T^4 := H^2(T) \tag{2}$$

To make things easier, one generally refers to the redshift z, instead of the scale factor a,

$$z = \frac{a_0}{a} - 1 \tag{3}$$

which corresponds to an increase in wavelength. We say that the early Universe had infinite redshift at the very beginning of the Universe, and that we have zero redshift today.

The cosmological principle implies that all quantities in the Universe are only

dependent on time t, and do not depend on position. It is assumed that the different forms of energies in the Universe can be described as perfect fluids in adiabatic expansions. There is considered to be no transfer of heat or mass. The different fluids in the Universe are matter that are made of a mixture of dark matter and baryonic matter. In the FLRW model, dark matter is considered as cold, with small velocities, so it is considered as non-relativistic particles. Dark energy is considered to be a cosmological constant, Λ with constant density and pressure, $\rho_\Lambda = -P_\Lambda$. This gives us the ΛCDM model were CDM stands for cold dark matter.

The Planck collaboration has made an updated list from 2018 of the observed values of the Hubble parameter and cosmological parameters of total matter, cold dark matter, baryonic matter, cosmological constant and curvature:

$$\begin{aligned} H_0 &= 67.66 \pm 0.42 \quad \text{km/s/Mpc} \\ \Omega_m &= 0.3111 \pm 0.0056 \\ \Omega_c h^2 &= 0.11933 \pm 0.00091 \\ \Omega_b h^2 &= 0.02242 \pm 0.00014 \\ \Omega_\Lambda &= 0.6889 \pm 0.0056 \\ \Omega_k &= 0.0007 \pm 0.0037 \end{aligned} \tag{4}$$

$h = H_0/100$ km/s/Mpc is the reduced Hubble parameter [6]. Since space is taken to be Euclidean for the FLRW metric, the curvature of the Universe is generally considered to be flat. Ω_k can be assumed to be zero. The different values for Ω explain the fraction of energies today. Ω is defined by the energy density of the given component over the critical density. If we use Ω_{coldDM} as an example, we have $\Omega_{coldDM} \equiv \frac{\rho_{coldDM}}{\rho_c}$, where $\rho_c \simeq (1.05h^2) \times 10^4 \text{eVcm}^{-3}$. We see that Ω_Λ, which is also called the fraction of dark energy, is taking up most of the energy in the Universe today. ΛCDM is defined by these six values listed in Eq.(4), and is therefore considered to obtain all cosmological data necessary [7]. Structure formation occurred mainly during the matter dominated era.
Most of the results in the Planck Collaboration are based on the cosmic microwave background, CMB. The CMB is microwave radiation that fill the Universe. In the early Universe the particles were charged with photons going through the plasma. Since the photons were thought to carry messages that were emitted at the recombination time, when atoms were created, they can still be observed in the CMB. These photons have had their wavelength redshifted and reduced by the expansion. After this the particles became stable and neutral, with bindings of a few eV. The CMB are said to be anisotropic, with fluctuations in temperature. The CMB is an important source of information since its properties can give constraints on scenarios describing the early Universe.

2.3 Standard Model

In Section 2.3 and 2.3.1 the theory is mostly based on chapter 11 and 12 from [8] with additional reference from [9] in Section 2.3.
Since 1978 the Standard Model has been the accepted theory of elementary particle physics and their interactions. In the Standard Model the fundamental particles are the leptons and quarks. All matter in nature is constructed from leptons, quarks, and the particles that mediate interactions between them. The force carriers are the photons, W and Z particles, eight types of gluons, and the Higgs boson. W stands for weak, and Z for zero because of weak and zero charge respectively. In Fig.1 we can see the masses, charges and spins for these elementary particles.

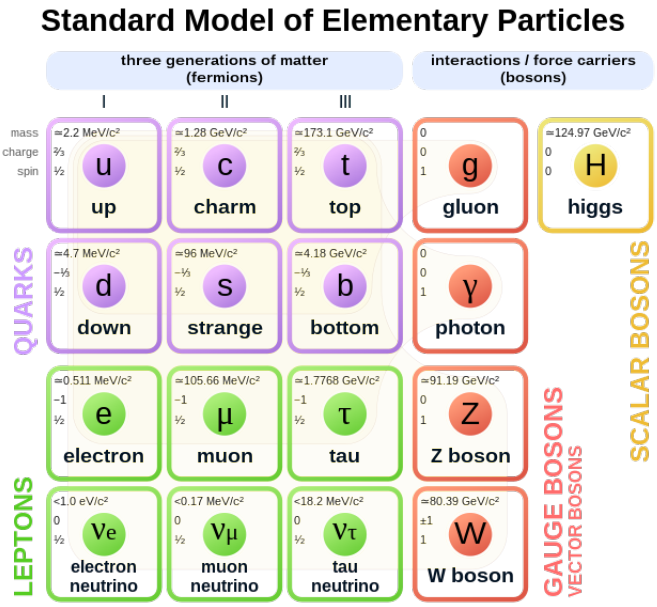

Figure 1: Mass, charge and spin of the elementary particles in the Standard Model. Figure taken from [10].

The Standard Model includes theories on the electroweak theory and quantum chromodynamics (QCD) which you can read more about in [8].

The quantum field theory requires that every particle has an antiparticle, with the same mass but opposite electric charge. Some particles, like the photon, can be their own antiparticle since they don't have charge. Dark matter particles should be chargeless, so we will assume that they are their own antiparticle when doing calculations in the sections about the thermal freeze out mechanism.

In the Standard Model, leptons are divided into electrons, muons and tau where all of them have their own neutrino. Neutrinos are both chargeless and stable so they could be a good candidate for dark matter particles. There are six different quarks where all of them have charge, and they can therefore not be dark matter particles. All these particles are listed in Fig.1.

The Standard Model contains three of the four known types of forces in Nature. These are the electromagnetic force, weak nuclear force, and the strong nuclear force. The range of force for strong interactions are about 10^{-15} m and about 10^{-18} m for weak force. The characteristic interaction time for strong interactions are only about 10^{-23} s, while for weak interactions it varies from about 10^{-16} s to about 10^{-10} s. Electromagnetic force is said to have infinite range with an interaction time of about 10^{-18} s. The gravitational force is also said to have infinite range, but is not included in the Standard Model. For lower energies the gravitational force has a range about 10^{-38} m, which is too weak to be observed in a laboratory.
The Standard Model combines the weak force and electromagnetic force into the electroweak theory. The Standard Model is identified by a high amount of symmetry. The reason that we can distinguish for example an electron from a neutrino is because of the so called spontaneous breaking of the symmetry. This is where the Higgs field contributes.
The broken symmetry results in a separation of the electromagnetic interaction made by the photon and the weak interaction made by the W and Z particles. We can see that the symmetry assumed in electroweak theory does not exist at lower energies because of the fact that the photon is massless and W and Z particles have masses in the order of 100 GeV/c^2. The Higgs boson is required for the symmetry-breaking agent called Higgs field. This boson was expected to have rest energy in the order of 1 TeV. When it was discovered in 2012 at the LHC the Higgs boson was set to be of mass equal to 125 GeV/c^2 [11]. According to the Standard Model, it is interaction with the Higgs field that give particles their masses.

Most of the everyday forces observed are due to electromagnetic interactions and occur between particles that all carry charge. Gravity also plays an important part, but as said earlier, it is so weak that it can be negligible in particle physics experiments. This is why it is not included in the Standard Model. Weak interactions happen between particles that carry weak charge. Strong interactions happen between particles that carry color charge. Some particles participate in more than one interaction, as for example the ones in electroweak theory.

Over a long period of time several particles have been considered to be elementary particles, and later discovered to be composed of several other particles. In addition to the different forces, the result of all these realizations is what we call the Standard Model. This has been a successful model in explaining and predicting the properties and interactions between particles. There are

continuously new understanding of the structure of matter, resulting in better understanding of particles as well.

The probability that an occurrence between two particles will create a reaction depends on the energies and what kind of particles are involved. The cross section is defined as

$$\sigma = \frac{R}{I} \tag{5}$$

where R is the number of reactions per unit time per particle, and I is the number of incoming particles per unit time per area, $\frac{\text{rate}}{\text{intensity}}$. Cross sections have the dimensions of area, usually in cm^2. The cross section can also be estimated with an approximate formula using the range, r of the interactions.

$$\sigma = \pi r^2 \tag{6}$$

From this we can see that the σ of strong interactions are $\sim 10^{-26}\text{cm}^2$, and for weak interactions $\sigma \sim 10^{-32}\text{cm}^2$. It is important to state that this is a really rough estimate. In reality we can see that for the weak interactions the cross sections are usually smaller, and they depend strongly on the energy of the interacting particles. We can see this fact in Fig.1 from [12]. The cross section ranges from 10^{-1}mb all the way down to 10^{-31}mb depending on the neutrinos energy. In cm^2 these values are between 10^{-28}cm^2 and 10^{-58}cm^2.

From [12], we can find that the cross section for an electron-neutrino scattering with an energy of a few GeV correspond to $\sigma \sim 10^{-13}$mb which is the same as $\sigma \sim 10^{-40}\text{cm}^2$. We take this as a typically weakly interacting scattering.

2.3.1 Beyond the Standard Model

After the successful unification of interactions into the electroweak theory there has been numerous efforts in unifying the strong interaction and gravitational interaction into one as well. The so-called grand unification theory, or GUT. Energies well below rest energy will lead to spontaneous symmetry breaking here as well. A new type of symmetry is included in the GUTs, called supersymmetry or SUSY. For each elementary particle explained from the Standard Model is given a superpartner, which is completely identical except for the spin. Leptons and quarks have spin 1/2, their superpartners have spin 0. Spin 1 particles have superpartners with spin 1/2. This makes a connection between fermions and bosons. For fermions, like for example the muons, the superpartners are called smuons. Bosons, like gluons, have superpartners called gluinos. If the superpartners were to have the same mass as their partnerparticle, they should have been detected a long time ago. Therefore, SUSY can suggest that the lightest superpartner would be very heavy, around the mass of W and Z particles.
In addition to high mass, many theories say that one of the superpartners are stable, electrically neutral and weakly interacting with the particles from the

Standard Model. This is all the requirements to form WIMPs, weakly interacting massive particles, that are proposed candidates for dark matter particles [13].

2.4 DarkSUSY

DarkSUSY is a flexible and modular Fortran code for precise calculations of many different indications and observables for dark matter. It is written by Joakim Edsjö, Torsten Bringmann, Paolo Gondolo, Piero Ullio and Lars Bergström, with contribution from several others as well. They have written a few articles explaining the tools and programs in DarkSUSY. I will use [14, 15] in this section when describing the tools I used since they are based on the latest edition, DarkSUSY 6.
The program was originally made for supersymmetric (SUSY) dark matter, but have later been updated to non-SUSY models as well. The program includes codes for relic density, direct and indirect detection and kinetic decoupling. For calculations in this thesis I used two different programs for a generic wimp module to calculate freeze out temperature, relic abundance and annihilation cross section multiplied by velocity for some different annihilation channels.

In the new release in 2018 new routines for calculating freeze out temperatures were included. Different ways of calculating direct and indirect detection were also improved. The generic WIMP model gives us the simplest example of a particle physics library in DarkSUSY. It gives us a picture of how DarkSUSY can be used to study the dark matter WIMP with the absolute minimum input of parameters. The parameters used are the mass of the dark matter, a decision whether the dark matter particle is its own antiparticle or not, a fixed annihilation cross section, which standard model particle the dark matter should mainly decay to, and the spin-independent scattering cross section with nucleons. Calculations in this thesis don't really care about the last one, so this is just put to 1pb everywhere. From these values the plots in the result section are obtained.

3 Evidence for Dark Matter

All of Section 3, about the evidence for dark matter, is mainly based on [1] and [16].
The first hint of the dark matter problem came in 1933. F. Zwicky found out that the mass of galaxies is much more than what the eye could see [8]. Evidence for dark matter can therefore be found in the invisible mass of galaxies, galaxy clusters, and also in even larger scales.
Observations from gravitational lensing reveal that dark matter is massive, stable over billions of years, very likely collisionless, interacting mostly gravitationally and separate from baryonic matter. We divide dark matter into hot dark matter with relativistic velocities and cold dark matter with non-relativistic velocities. Neutrinos are particles in the Standard Model with relativistic speed and can fit the hot dark matter description. They fit the description because they are chargeless, they have mass and they are so light that they have relativistic speeds. Hot dark matter is composed of massive and high velocity components, and it tends to spread structures such as galaxies. This matter makes the structure of a galaxy quite different than what we can see. This leads to the fact that hot dark matter can only be a small part of the total dark matter, and that most of the dark matter in the Universe should be cold. Cold dark matter can be everything from weakly-interacting massive particles of new physics models to primordial black holes already existing in the early Universe.

The existence of dark matter relies on the observations of gravitational effects in large-scale structures and in cosmology. In section 5 is given some search techniques for dark matter which does not use this gravitational effect. In the following subsections we will look at evidence for the existence of dark matter in galaxies, galaxy cluster, and at larger cosmological scales.

3.1 Galaxies

In galaxies the evidence lies particularly in spiral galaxies. Rotation curves of galaxies are the most convincing and direct evidence for dark matter on galactic scales. Here, most of the visible mass is gathered in the budge and the disc. These are centred quite in the middle, so far from here the disc fades away. Now, the star density decreases, the total mass inside the visible radius becomes constant and the velocity is also expected to decrease. Using Gauss´ theorem, we can see this since the velocity of stars v at the distance R from the galactic centre is:

$$v(R) = \sqrt{\frac{GM(R)}{R}}. \tag{7}$$

The observed velocity far from the centre of the spiral galaxies has actually been approximately constant. With constant velocity, the mass continues increasing far beyond the fading of the visible disc. The distribution of dark matter is measured by the observations of rotation velocities of distant stars and gas clouds around the galaxies [2]. Globular clusters are found in the galactic halo,

that extend well beyond the visible disc. Globular clusters are gravitationally bound groups of stars, and are known to have small amount of dark matter, since they are a part of the halo [17]. Most of the matter in the halo is invisible, and its mass is therefore considered to be dark matter. Globally dark matter seems to represent about $80\% - 90\%$ of the total mass of galaxies.

3.2 Galaxy clusters

Galaxy clusters are clusters of galaxies, and of course very massive objects which contain large quantities of gases in the intergalactic medium. These gases can reach high velocities and emit X-ray. Analysis of the emitted X-ray together with a modeling of the galaxy clusters were used to weigh the total mass of the clusters. This mass was compared to the visible mass, resulting in a large fraction of invisible mass. Even though the evidence was there, the models were criticized for their approximation. Therefore, these methods have been replaced by gravitational lensing. This is a method where we observe the deformed image of distant objects and reconstruct the path of the light. Gravitational lensing is often used to weigh galaxy clusters. These studies tend to show that visible mass only represent about $10\% - 20\%$ which is similar to what is found in galaxies as well.

The Bullet Cluster 1E0657-558 can be considered as a breakthrough for understanding the nature of dark matter. The major part of the mass is separated from the hot visible gas and therefore proves that baryonic mass and dark matter are separate from each other [2]. Fig.2 is of the Bullet Cluster 1E0657-558 and shows that it is actually composed of two galaxy clusters that collided. The collision of the galaxies makes direct detection of dark matter a possibility. During the collision the structures of the galaxies decoupled from the plasma and got a separation between the main cluster and subcluster of 0.72 Mpc. The bullet shape is due to the drag force on the hot gas caused by interactions during the collision [18].

3.3 Large-scale structures

The problem of dark matter extends to larger and cosmological scales. Via gravitational collapse in the denser regions matter starts gathering and leads to forming of large-scale structures in which galaxies also appear. There are two main things that affect the structures. Gravitational interaction that attracts matter in the centres, and the expansion of the Universe drives structures away from each other. Simulations of these structures have been used to study the interactions between expansion and gravity and also to study the role of dark matter in this process. Contrary to baryonic matter, dark matter is generally considered as collisionless. We can therefore distinguish these particles from each other in the simulation. It is possible to compare the simulated data with observed data by using precise statistical analysis to analyze the data set. To get this similarity the power spectrum is used. This is a spectrum showing the

Figure 2: Observation of the Bullet Cluster 1E0657-588. The pink is hot gas, the visible mass, observed by the Chandra X-ray Observatory, while the blue is the major part of the mass made from gravitational lensing. So the blue is considered to be the dark matter mass. Figure copied from [1] with permission from Elsevier.

distribution of different spreads of structure and regions in the CMB [19]. The Planck Collaboration has made such a power spectrum which correspond well with the Planck results from Eq.(4). Therefore, the Planck results are in good agreement with the large-scale structure data, and also in agreement with the results of galaxies and galaxy clusters concerning ratio of baryonic mass over the total mass.

3.4 Dark matter properties

The main requirements for particles to be good candidates for cold dark matter are that they have to be massive with non-relativistic speed and stable over tens of billions of years. These are not considered to be particles in the Standard Model. The most common method in achieving stability, is to have a discrete symmetry to protect particles. Under a Z_2 symmetry, new physics particles have a multiplicative charge -1, the Standard Model have charge +1. New particles can only decay into an odd number of new particles in addition to standard particles, and they can (co)-annihilate into Standard Model particles. The lightest new particles are stable, can be produced by collisions of Standard Model particles, and can annihilate inside dark matter halos. These halos are mostly made of invisible matter around galaxies and galaxy clusters, as explained earlier in Section 3 about the evidence. The surviving dark matter particles are called relics. In a complete scenario it is possible to compute the relic abundance of dark matter. We have both thermal relics and non-thermal relics for this purpose.

4 Thermal freeze out and relic density

We are going to assume that the particles are produced by a mechanism called thermal freeze out. This mechanism is assumed to happen when radiation was the dominant energy in our Universe.

4.1 Theory of thermal freeze out

Thermal relics are relics where the new particles were in thermal equilibrium in the early Universe. In equilibrium the distribution functions of the new particles can either be Fermi-Dirac (fermions) or Bose-Einstein (bosons). These distributions are a bit different from each other. Since the temperature is extremely high in the early Universe, we can just reduce both distributions to the Boltzmann distribution instead:

$$f_i(E_i, T) = g_i \exp\left(-\frac{E_i}{T}\right) \tag{8}$$

where g_i is the degeneracy and T is measured in GeV [1].
The particles are made in the early Universe, the interaction between the particles is weak, and the chemical potential is taken to be negligible. Chemical potential is a quantity describing the tendency for particles to interact. It depends on different things like for example state, temperature and pressure [20]. Since the Universe is in expansion, the average distance between particles can increase, and the equilibrium can be broken. The unstable particles decay and the stable ones undergo a freeze out. Their number is frozen and nearly constant.

We can use relic density computed within a given model to limit our dark matter scenarios. The results from these models can be compared to the observed cosmological dark matter density [1].
We will now perform the calculation of relic density for the mechanism called thermal freeze out with derivations based on [5]. It is assumed that the dark matter particle χ is its own antiparticle. For the freeze out, we assume that it only happens when the particle is non-relativistic and in thermal equilibrium. This is so we can approximate the equilibrium distributions of both the SM particle, f, and the DM particle, χ by simple Boltzmann factors.
In many new physics scenarios only one particle becomes stable and can form dark matter. If considering a standard case where the dark matter is made of one single type of particles, and the new physics particles are protected by a discrete symmetry so that new particles are produced in pair, we can compute the relic abundance. The computation of the relic abundance is based on solving the Boltzmann evolution equation.

$$\frac{dn_\chi}{dt} + 3Hn_\chi = -\langle\sigma v\rangle(n_\chi^2 - n_{\chi eq}^2), \tag{9}$$

where n is the number density of the new physics particle, n_{eq} its equilibrium density given by

$$n_{eq} = g_i \left(\frac{m_i T}{2\pi} \right)^{3/2} \exp^{-m_i/T}, \tag{10}$$

and $\langle \sigma v \rangle$ is the thermal average of the annihilation cross section of the new physics particles to Standard Model particles multiplied by their relative velocity.
From Eq.(9) we can rewrite the Boltzmann equation by defining the yield, Y_χ to be dependent on the number density n_χ and entropy, s.

$$Y_\chi := \frac{n_\chi}{s} \tag{11}$$

where s is the entropy density of the thermal plasma,

$$s = \frac{2\pi^2}{45} g_{*s} T^3, \tag{12}$$

g_{*s} is approximately the number of relativistic degrees of freedom in the cosmological plasma. For the temperatures relevant for dark matter freeze out, g_{*s} is considered to be equal to g_*, which can be seen in Fig.5. Because of the expansion of the Universe, the entropy per comoving volume is conserved, therefore $sa^3 = const$. With this it follows that,

$$\frac{dn_\chi}{dt} + 3Hn_\chi = s\frac{dY_\chi}{dt} \tag{13}$$

Combining Eq.(9) and Eq.(11) we can rewrite Eq.(9) as

$$\frac{d(sY_\chi)}{dt} + 3HsY_\chi = -\langle \sigma v \rangle (s^2 Y_\chi^2 - s^2 Y_{\chi eq}^2) \tag{14}$$

Then we can separate the derivatives of the entropy and the yield variable, and $\frac{ds}{dt}$ just becomes $-3sH$, and we end up with,

$$\frac{dY_\chi}{dt} = -\langle \sigma v \rangle s (Y_\chi^2 - Y_{\chi eq}^2) \tag{15}$$

We can take $x = \frac{m_\chi}{T}$ to replace t. Since we want to get the yield derivative dependent on x and not t, we introduce this independent variable that proves to be more convenient. To find t as a variable of x we can use Eq.(2) defined in the section about expansion.
Rewrite Eq.(2) so we get a function for t, change T to $\frac{m_\chi}{x}$ and take $\frac{dt}{dx}$

$$\frac{dt}{dx} = \frac{\sqrt{90} x M_{Pl}}{\pi \sqrt{g_*} m_\chi^2} \tag{16}$$

We can use the relation that,

$$\frac{dY_\chi}{dx} = \frac{dY_\chi}{dt}\frac{dt}{dx} \tag{17}$$

to find $\frac{dY_\chi}{dx}$, so we end up with

$$\frac{dY_\chi}{dx} = -\langle\sigma v\rangle s(Y_\chi^2 - Y_{\chi eq}^2)\frac{\sqrt{90}xM_{Pl}}{\pi\sqrt{g_*}m_\chi^2} \tag{18}$$

If we expand Eq.(16) by x we get $\frac{1}{Hx}$ and we get our final result for the Boltzmann equation in terms of Y_χ and x,

$$\frac{dY_\chi}{dx} = -\frac{xs}{H(m_\chi)}\langle\sigma v\rangle(Y_\chi^2 - Y_{\chi eq}^2) \tag{19}$$

In order to get $H(m_\chi)$ we have to use the relation $H(T) = x^{-2}H(m_\chi)$.

We can remake Eq.(19) by using the value for collision rate, which is $\Gamma = n_{\chi eq}\langle\sigma v\rangle$.

$$\frac{x}{Y_{\chi eq}}\frac{dY_\chi}{dx} = -\frac{\Gamma}{H(T)}\left[\left(\frac{Y_\chi}{Y_{\chi eq}}\right)^2 - 1\right] \tag{20}$$

Γ and H can therefore be expected to be comparable to some order of unit at freeze out.
We can also define x_{fo} to be at the point where, $H = \Gamma k = \langle\sigma v\rangle n_{\chi eq}k$, where k is some constant of order unity. x_{fo} can be estimated by [5]

$$x_{fo} \simeq \ln\Big[C(n+1)\Big] - (n+1)\ln\Big(\ln\Big[C(n+1)\Big]\Big) \tag{21}$$

where $C = \sqrt{\frac{90}{8\pi^3}}(g_\chi/g_*^{1/2})m_\chi M_{\rm Pl}\sigma_n$.
Since we assume a non-relativistic particle, the temperature is already below the dark matter mass. The freeze out happens when the Universe expand even more, so the temperature drops even more. Then the annihilation process is less important, and the Hubble term becomes larger than the right side of Eq.(9), and approximately equal to the collision rate Γ. When $\Gamma \gtrsim H$, the dark matter particles are still coupled, so still in thermal equilibrium. When $\Gamma \lesssim H$, the particles have been through freeze out, and they have decoupled.
Before this happens, the number density will follow the equilibrium value. The annihilation process is not efficient anymore when the particle departures from equilibrium. The temperature is now referred to as the freeze out temperature, T_{fo}. This temperature depends on the value of the average annihilation cross section. Larger cross sections lead to smaller freeze out temperatures. This is because the dark matter mass stays longer in thermal equilibrium before freeze out when the cross section is bigger. We can see this in Fig.3.

We can now use Eq.(19) to determine the relic abundance, $\Omega_\chi h^2$. We want to find Y_χ long after freeze out happens, so we can neglect $Y_{\chi eq}$. For simplicity, we can assume that $\langle\sigma v\rangle \simeq \sigma_n x^{-n}$, and use the formula for our entropy, s from Eq.(12).

$$\frac{dY_\chi}{dx} = -\frac{xg_{*s}2\pi^2 m_\chi^3 x^{-3}}{45H(m_\chi)}\sigma_n x^{-n}Y_\chi^2 \tag{22}$$

We can take all the constants into one to make the equation simpler.

$$\lambda = \frac{g_{*s} 2\pi^2 m_\chi^3}{45 H(m_\chi)} \tag{23}$$

Then Eq.(22) can be written as:

$$\frac{dY_\chi}{dx} = -\lambda \sigma_n x^{-n-2} Y_\chi^2 \tag{24}$$

When this equation is integrated between x_{fo} and $x_0 \simeq \infty$, it gives us,

$$Y_\chi \simeq \frac{(n+1) x_{fo}^{n+1}}{\lambda \sigma_n} \tag{25}$$

In Fig.3 we have plotted the yield at equilibrium and the actual yields against x to see where the freeze out happens for different annihilation cross sections. For this figure the annihilation channel for muon is used with WIMP mass=100 GeV. The particle is also considered to be its own antiparticle. As mentioned above, freeze out happens later for larger cross sections. In Fig.3 we see that freeze out for $\langle \sigma v \rangle = 10^{-27} \text{cm}^3/\text{s}$ happens before freeze out for the other two $\langle \sigma v \rangle$.

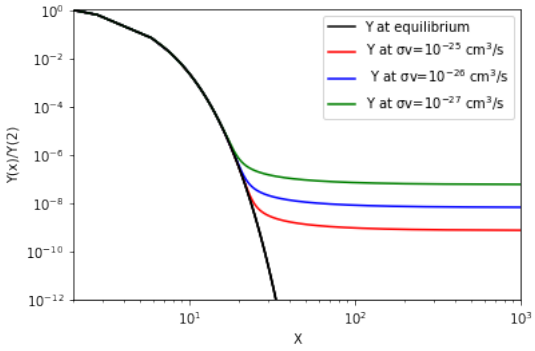

Figure 3: The yield plotted against x with different annihilation cross sections with muons as main annihilation channel.

To convert Eq.(25) to the relic abundance, $\Omega_\chi h^2$ we can multiply it by $\frac{m_\chi s_0}{\rho_c}$. We also change σ_n back to $\langle \sigma v \rangle$ so we get $\frac{\langle \sigma v \rangle}{x_{fo}^{-n}}$.

$$\Omega_\chi \simeq \frac{(n+1) x_{fo}^{n+1}}{\lambda \langle \sigma v \rangle x^n} \frac{m_\chi s_0}{\rho_c} \tag{26}$$

Change back λ, $H(m_\chi)$ and T to get the final result,

$$\Omega_\chi \simeq \frac{45\sqrt{g_*}\pi m_\chi^2}{2\pi^2 M_{Pl}\sqrt{90}} \frac{(n+1) x_{fo} m_\chi s_0}{g_{*s} m_\chi^3 \langle \sigma v \rangle \rho_c} \tag{27}$$

After making Eq.(27) prettier we are left with,

$$\Omega_\chi \simeq \frac{45 s_0}{\sqrt{90} 2\pi \rho_c} \frac{(n+1)x_{fo}}{M_{Pl} \frac{g_{*s}}{\sqrt{g_*}} \langle \sigma v \rangle} \tag{28}$$

Measurements give $s_0 \simeq 3000\text{cm}^{-3}$ and $\rho_c \simeq (1.05h^2) \times 10^4 \text{eVcm}^{-3}$.

$$\Omega_\chi h^2 \simeq \frac{45 \times 3000\text{cm}^{-3}}{2\pi(1.05 \times 10^4 \text{eVcm}^{-3})\sqrt{90}} \frac{(n+1)x_{fo}}{M_{Pl} \frac{g_{*s}}{\sqrt{g_*}} \langle \sigma v \rangle} \tag{29}$$

$$\Omega_\chi h^2 \simeq 0.216 \times 10^9 \text{GeV}^{-1} \frac{(n+1)x_{fo}}{M_{Pl} \frac{g_{*s}}{\sqrt{g_*}} \langle \sigma v \rangle} \tag{30}$$

Eq.(30) gives us an approximate solution for the relic abundance, dependent on x_{fo}, $\langle \sigma v \rangle$ and g_*. We can see that when the $\langle \sigma v \rangle$ gets bigger the $\Omega_\chi h^2$ gets smaller. From this we can see that the relic abundance, the quantity of relics remaining, is smaller if the $\langle \sigma v \rangle$ is larger. The decrease in relics left is logical because of the fact that the dark matter stays longer in thermal equilibrium for larger cross sections, as already mentioned.

4.2 DarkSUSY results

Our assumption on the dark matter particles in the early Universe in the generic wimp module is that they annihilate to some type of Standard Model particles. We have performed some calculations using full DarkSUSY codes briefly mentioned in section 2.4, DarkSUSY.
We will now check whether these correspond to our approximate result from Eq.(30). When doing these calculations we will see that, indeed, dark matter produced via thermal freeze out must have cross sections of the order typical for weak interactions. We have made plots comparing WIMP mass with the freeze out x, relic abundance and annihilation cross section multiplied by velocity. We have chosen muons and neutrinos to be the annihilation channels the dark matter particles mainly decay into.
The relic abundance in Eq.(30) depends on the particle f that is obtained through freeze out only through $\langle \sigma v \rangle$. This quantity will be fixed in our calculations using DarkSUSY, hence, we don't expect any further dependence on our annihilation channel chosen for particle f. The relic abundance depends on the dark matter mass through x_{fo}. Since the mass only has logarithmic dependence in x_{fo}, it also depends very weakly on the final result for the abundance.

To get the plots in Fig.4, Fig.6 and Fig.7 the program called dsmain_wimp in DarkSUSY was modified so it only depended on the simple module considering the generic wimp. From this program data sets were made with WIMP mass, Ωh^2 and x_{fo} for the different cross sections and annihilation channels plotted.

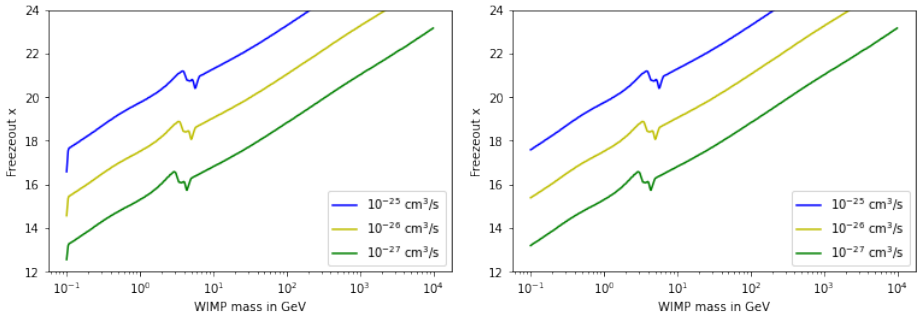

(a) Muons as main annihilation channel (b) Neutrinos as main annihilation channel

Figure 4: Freeze out x for the two main annihilation channels chosen

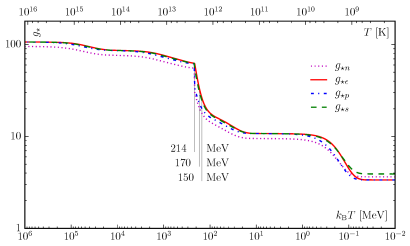

Figure 5: Evolution of g_* and g_{*s}, Figure copied from [21]. Our g_* is plotted as $g_{*\epsilon}$ in this figure.

In Fig.4 is plotted where freeze out happens compared to WIMP mass for the three different cross sections chosen. Values were used where the dark matter was assumed to annihilate mainly into muons and neutrinos respectively. It can be seen that they have quite similar behaviour except at the very beginning since muons are heavier than neutrinos. This is why the annihilation process cannot start as early here as for the neutrinos. The dark matter mass has to become larger than the particle it is decaying into before it can annihilate. By looking at this plot we see that it has a linear graph in logarithmic scale on the axis with mass. This confirms what was shown in Eq.(21), that the mass only depends logarithmicially on x_{fo}. One can also observe that there is a small bump in the plot. When looking at the values obtained from DarkSUSY, we see that this bump happens when WIMP mass is around 4 GeV. This corresponds to Fig.5, where we can see a change in the relativistic degrees of freedom, g_*, at $T = 0.2$GeV. Using $x = \frac{m_\chi}{T}$ we see that these values match.

In Fig.6 we have a plot where the WIMP mass is plotted against the relic abundance with the same cross sections chosen in DarkSUSY as for x_{fo}. The measured value of $\Omega_c h^2$ from Eq.(4) is included for comparison, with an error of 3σ. This tells us that the correct value of cross section probably is between

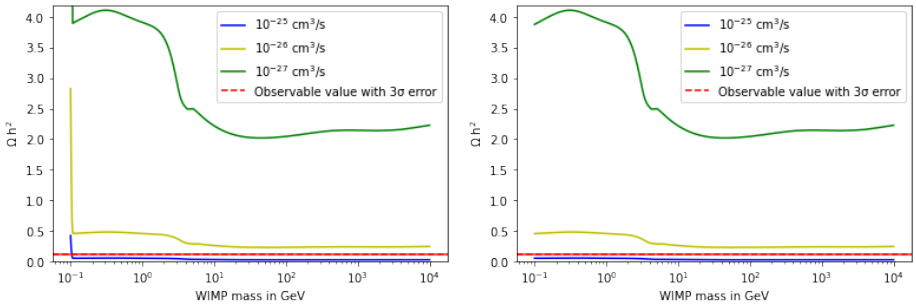

(a) Muons as main annihilation channel (b) Neutrinos as main annihilation channel

Figure 6: Relic abundance for the two main annihilation channels chosen

10^{-25}cm^3/s and 10^{-26}cm^3/s.

Fig.7 is also a plot with mass plotted against the relic abundance with 3σ

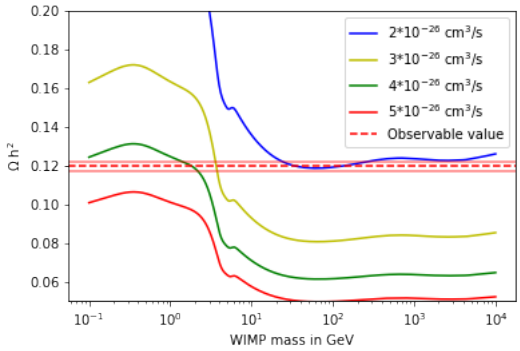

Figure 7: Relic abundance at different annihilation cross sections compared to observed value from Eq.(4) with neutrinos as main annihilation channel

error on the measured value. This time it was made with the intention of finding the best value for the cross section compared to the measured value from the Planck Collaboration. Since we assume the WIMP particle to be massive, maybe around 100 GeV, we can see that the best fitted value for $\langle\sigma v\rangle$ is 2×10^{-26}cm^3/s.

For Fig.8 the program called oh2_generic_wimp was used. In this program the $\Omega_c h^2$ was updated to the value from the Planck Collaboration noted in Eq.(4) with 3σ errors. It was also modified so the data set used to make the plot included $\langle\sigma v\rangle$ for both muons and neutrinos in addition to tau and W. In Fig.8 is shown what $\langle\sigma v\rangle$ that is required to obtain a correct dark matter relic abundance for different masses. In this plot is shown separately the cases where dark matter annihilates mainly to $\nu_e\bar{\nu_e}$, $\mu^+\mu^-$, $\tau^+\tau^-$ and W^+W^-. If the dark

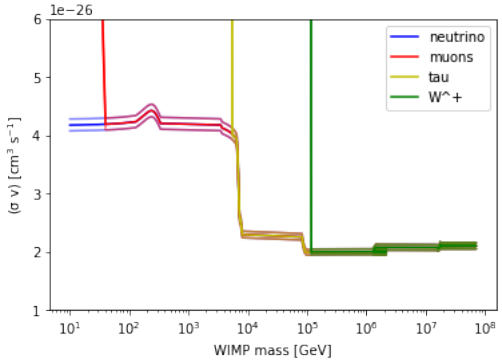

Figure 8: Annihilation rate for different masses

matter mass is below the kinematic threshold, the cross section drops to zero. We can see that this happens for the W^+W^- particles. Since they are heavy particles, the dark matter mass has to be quite large for freeze out to happen. Neutrinos are the lightest, so freeze out can happen for smaller dark matter masses that annihilate into neutrinos. We see that freeze out into muons happens right after neutrinos. We can relate this to what we saw in Fig.4, that the freeze out could not start quite as early for muons as for neutrinos. Apart from this effect, the non-constant part of the cross section is only due to changes in the effective number of relativistic degrees of freedom [15]. We can understand this from Eq.(30),

$$\Omega_\chi h^2 = \# \frac{x_{fo}}{\frac{g_{*s}}{\sqrt{g_*}}\langle\sigma v\rangle} \tag{31}$$

The correct relic abundance is obtained for about $x_{fo} \sim 20$ for all dark matter masses. g_{*s} is related to the entropy density, while g_* is related to energy density. In Fig.5 the number of relativistic degrees of freedom relevant for energy density is denoted as $g_{*\epsilon}$. As mentioned before, $g_{*s} = g_*$ for temperatures relevant for dark matter freeze out. We can take,

$$\frac{g_{*s}}{\sqrt{g_*}} \sim \sqrt{g_*}\Big|_{x=x_{fo}} \sqrt{g_*}\Big|_{x\sim 20 \Rightarrow T\sim\frac{m_\chi}{20}} \tag{32}$$

From Fig.5 we can see that there is a change in g_* at $T \sim 0.2$GeV which gives us $m_\chi \sim 4$GeV. This can also be seen, as mentioned, in Fig.4.

$$T > 0.2\text{GeV} \qquad T < 0.2\text{GeV} \tag{33}$$
$$g_* \sim 100 \qquad g_* \sim 10 \tag{34}$$
$$m_\chi > 4\text{GeV} \qquad m_\chi < 4\text{GeV} \tag{35}$$

To keep the relic abundance constant we have to increase $\langle \sigma v \rangle$ by a factor of $\sqrt{\frac{100}{10}} \sim 3$.

We can use Eq.(30) and our values obtained from DarkSUSY, which are plotted in Fig.4 and Fig.6 to check if the formula and the values based on full calculations using DarkSUSY agree. Since our setup in DarkSUSY is based on the generic wimp module, we can set $n = 0$ and $M_{\text{Pl}} \simeq 2.4 \times 10^{18}\text{GeV}$ for all calculations. x_{fo} have different values depending on which WIMP mass we choose to look at, and at what cross section. g_* also depends on this mass, since it depends on temperature, as we can see from Fig.5. Since our final answer is dimensionless, we need to find $\langle \sigma v \rangle$ in units of GeV^{-2} so it cancels out with our constant and Planck mass in Eq.(30). Usually $\langle \sigma v \rangle$ is measured in units of cm^3s^{-1}. We can use the fact that in particle physics we always take $\hbar = c = 1$. This gives us:

$$\hbar = 6.582 \times 10^{-16}\text{eVs} = 1 \qquad \text{and} \qquad c = 2.9979 \times 10^8\text{m/s} = 1 \tag{36}$$

We can use these relations to say that

$$1\text{s} = \frac{1}{6.582 \times 10^{-16}\text{eV}} \tag{37}$$

and

$$1\text{m} = \frac{1\text{s}}{2.9979 \times 10^8} = \frac{1}{2.9979 \times 10^8 \times 6.582 \times 10^{-16}\text{eV}} = \frac{1}{1.973 \times 10^{-7}}\text{eV}^{-1} \tag{38}$$

which gives us

$$1\text{m} = 5.068 \times 10^6\text{eV}^{-1} \qquad \text{and} \qquad 1\text{cm} = 10^{-2}\text{m} = 5.068 \times 10^4\text{eV}^{-1} \tag{39}$$

Since we want to find $\frac{\text{cm}^3}{\text{s}}$, we can convert this to $\frac{\text{cm}^2 \times 10^{-2}\text{m}}{\text{s}} = \text{cm}^2 \times 10^{-2} \times \frac{1}{2.99979 \times 10^8}$, and now the only thing left to do is to square Eq.(39).

$$1\text{cm}^2 = 2.5689 \times 10^9\text{eV}^{-2} = 2.5689 \times 10^9 \times (10^9)^2\text{GeV}^{-2} = 2.5689 \times 10^{27}\text{GeV}^{-2} \tag{40}$$

Now the units for our $\langle \sigma v \rangle$ has changed from cm^3s^{-1} to GeV^{-2}.

$$\frac{\text{cm}^3}{\text{s}} = 2.5689 \times 10^{27}\text{GeV}^{-2} \times 10^{-2} \times \frac{1}{2.99979 \times 10^8} \tag{41}$$

Now we have all the values needed to calculate different relic abundances for different WIMP masses at wanted cross sections. If we take our mass to be

100 GeV, it corresponds to $x_{fo} = 21.02825$ for $\langle\sigma v\rangle = 10^{-26}\text{cm}^3\text{s}^{-1}$. Since $T = \frac{m}{x}$ we get $T \sim 5\text{GeV}$, and we can see from Appendix A in [21] that $g_* = 85.60$. These are the values we use in Eq.(42), when writing out Eq.(30). For WIMP mass=10 GeV we get $g_* = 69.26$. For WIMP mass=1000 GeV, $g_* = 97.40$. For WIMP mass=0.1 GeV, $g_* = 10.76$ and for WIMP mass=10 000 GeV, $g_* = 106.61$. So, for WIMP mass=100 GeV and $\langle\sigma v\rangle = 10^{-26}\text{cm}^3\text{s}^{-1}$, we get

$$\Omega h^2 = 0.216 \times 10^9 \text{GeV}^{-1} \times \frac{21.02825}{2.4 \times 10^{18}\text{GeV} \times \sqrt{85.60} \times 10^{-26} \times 2.5689 \times 10^{27}\text{GeV}^{-2} \times 10^{-2} \times \frac{1}{2.99979 \times 10^8}} \tag{42}$$

Using Jupyter Notebook this equation gives us a relic abundance of 0.2387 where our result from DarkSUSY is 0.2301, which results in an error of about 3.6%. One can also try WIMP mass=100 GeV for $\langle\sigma v\rangle = 10^{-25}\text{cm}^3\text{s}^{-1}$ and $\langle\sigma v\rangle = 2\times10^{-26}\text{cm}^3\text{s}^{-1}$, which we can see from our plots also should give approximately correct values. Using the formula, these annihilation cross sections give us a relic abundance of 0.0264 and 0.1232 respectively. Using $\langle\sigma v\rangle = 10^{-25}\text{cm}^3\text{s}^{-1}$, we got a value for Ωh^2 with an error of 3.0%, and an error of 3.5% when trying for $\langle\sigma v\rangle = 2 \times 10^{-26}\text{cm}^3\text{s}^{-1}$. I also tried calculating for different WIMP masses, where the values turned out to be more accurate for WIMP mass around 1000 GeV compared to 10 GeV. WIMP mass=1000 GeV actually gave smaller error than 100 GeV as well, for all three $\langle\sigma v\rangle$. Trying for example 10 000 GeV gave larger error again. Overall, the obtained formula for relic abundance is quite good, and gives approximately correct answers for given values compared to what is given by DarkSUSY calculations. If we compare to the measured value from the Planck Collaboration, which says that $\Omega_c h^2 = 0.11933 \pm 0.00091$, which is the value I inserted in Fig.7, with 3σ error, we can see both from the plot and from values obtained from the formula that $\langle\sigma v\rangle = 2 \times 10^{-26}\text{cm}^3\text{s}^{-1}$ could be the most probable value for annihilation cross section, if we were to fix it to some value. This value fits best for most WIMP masses.

If we take $\langle\sigma v\rangle$ to be $10^{-26}\text{cm}^3/\text{s}$ for simplicity, and choose $v = 0.1c$, we can find a typical value for the cross section σ. We choose a velocity of $0.1c$ because this is the expected velocity of particles in the early Universe around freeze out.

$$\sigma \sim \frac{10^{-26}\text{cm}^3/\text{s}}{0.1 \times 3 \times 10^8 \times 10^2\text{cms}^{-1}} \sim 10^{-36}\text{cm}^2 \tag{43}$$

This cross section is around the same order of magnitude as the cross section for weak interactions calculated in Section 2.3 Standard Model. Since these cross sections correspond well, we can assume that the weakly interacting particles explaining the WIMP miracle could be a good example for a dark matter particle. This is if we take thermal freeze out to be a correct mechanism for calculating dark matter particles.

5 Search for dark matter particles

Section 5, about experiments in the search for dark matter particles, are based on [1].
Today, dark matter is still a hot topic and actively searched for. Both direct and indirect detection are used, and dark matter is also searched for in colliders. Interactions between particles in the Standard Model can be described by Feynman diagrams shown in Fig.9b. They are space-time diagrams, where ct is plotted against the x graphs. They can be used to compute lifetimes and cross sections [8]. In Fig.9a the different detection searches between dark matter particles and Standard Model particles are shown. Their interactions are set to happen in the grey circle. Either as direct detection where the dark matter particle interact with the Standard Model particle, and give a dark matter particle and a Standard Model particle, or by indirect detection where they interact and decay into Standard Model particles. Colliders search for dark matter by going in reverse, from Standard Model particles to the dark matter particles.
The two figures in Fig.9, show two types of Feynman diagrams. Fig.9a show a Feynman diagram with the different types of detection where the arrows indicate the direction of time, while Fig.9b is an example of a Feynman diagram where an electron and a positron interact and annihilate into two photons. This indicate that the dark matter particles should interact in the same way with Standard Model particles as the SM particles do with each other. If we assume that thermal freeze out is the correct mechanism for dark matter production, the interactions represented in Fig.9a should appear as well.

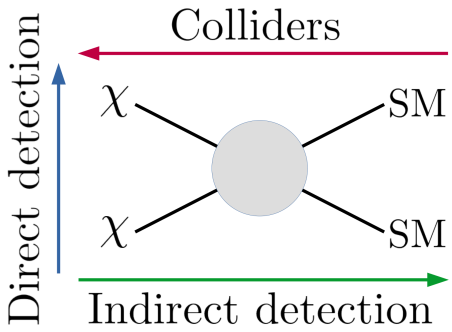

(a) Figure copied from [1] with permission from Elsevier.

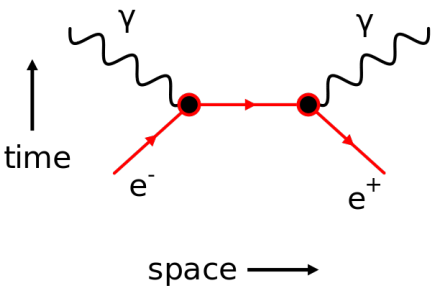

(b) Figure taken from [22].

Figure 9: In the figure on the left, the three different types of dark matter particle searches are shown by a Feynman diagram. The arrows indicate the direction of time. On the right side, Feynman diagram where an electron and a positron annihilate into two photons are shown.

5.1 Direct detection

In addition to [1], Sections 5.1 and 5.2 are also based on [16].
Density of dark matter in our Solar System is found to be about $0.4\text{GeV/cm}^3 = 400000\text{GeV/m}^3$. It is determined by looking at the rotation curves of the Milky Way. If we assume dark matter particles around 100 GeV in mass, we have about 4000 dark matter particles per cubic metre in the Solar System. Since the galactic halo is fixed compared to the disc that is rotating, and dark matter is considered to be in the halo, we assume a relative velocity of 200 km/s=200 000m/s for the dark matter particles. We can calculate the amount of dark matter particles per cubic metre per year by $1\text{m}^2 \times 200000\text{m/s} \times 1\text{year} \times 4000\text{particles per cubic metre} = 2.5 \times 10^{16}$. Looking for these particles is an excellent way of searching for dark matter interactions.
Large tanks and detectors of specific materials can be made to maximize the probability of interaction. Experiments tried in these detectors can make the dark matter and standard matter interact via scatterings with the particles present. The recoil energy can then be measured and used to find approximate amount of dark matter mass. The cross section can also be measured from this. Direct detection is probably the most promising way of detecting dark matter. Even though the estimated dark matter particles can be measured, the particles themselves are yet to be seen and observed. We can see some different results of direct detection experiments in Fig.10. In these results it is assumed that dark matter is made of a single type of WIMP. The solid lines are exclusion limits for the results from the different experiments. This indicates a smaller σ needed for heavier dark matter masses. The dashed lines are some potential limits for future experiments. We see that the cross sections of the dark matter with the nucleon is as low as $\sim 10^{-46}\text{cm}^2$ for dark matter mass around 10-100 GeV when looking at the lowest solid line. These results tell us that the WIMP miracle with a $\sigma \sim 10^{-36}\text{cm}^2$ might not be correct, and you could argue that the mechanism used for thermal freeze out is wrong. By looking at Fig.10, the possibility that dark matter might be a lighter particle than assumed in the WIMP miracle should also be considered. We see that the cross section needed for dark matter mass of 1 GeV is not as small as the ones needed for masses of 100 GeV.

5.2 Indirect detection

Indirect detection is a different experiment in the search for dark matter. It is a technique of observing the radiation produced in dark matter annihilations. So, these experiments look at the production of Standard Model particles through dark matter interactions or decay. Then they are detected on Earth or for example in dense regions of galactic halos. There are different types of experiments depending on the particle searched for. Photons, charged particles and neutrinos are the most common products. As can be seen in Fig.9a, dark matter can interact and make Standard Model particles. When two dark matter particles are close to each other, they can interact and annihilate into Standard Model

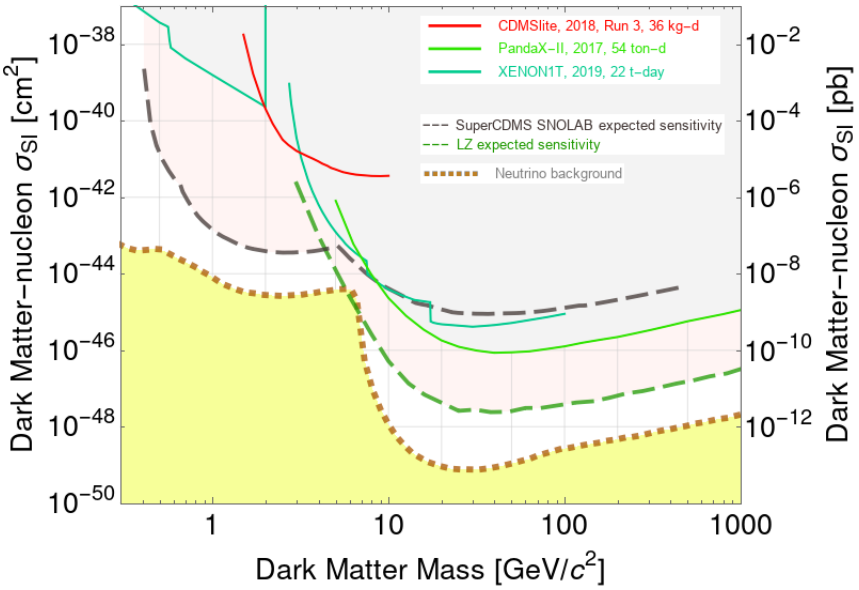

Figure 10: Results from experiments used in search for dark matter particles with direct detection. The solid lines are exclusion lines from experiments already done, while the dashed lines are possible limits for experiments planned. The yellow region is the cosmic neutrino background. Figure copied from [1] with permission from Elsevier.

particles. For this to happen, there has to be a small binding between the two parts. These interactions have different probabilities of happening depending on the relative velocity between dark matter particles and on the annihilation cross section into SM particles.

5.3 Collider searches

New physics scenarios can be directly searched for at particle colliders, and in particular at the LHC, large hadron collider. The colliders study new physics scenarios by wanting to make new particles with high energy collisions, or to make heavy particles which in turn decay into the new particles. The Higgs boson can be an example of such a heavy particle decaying into smaller new particles not detected yet. The main challenge in the search for dark matter is that the particles are expected to be neutral, uncoloured and weakly interacting. The couplings to the Standard Model particles are therefore small. The only way to detect the dark matter particles produced in a collider is to look at the partner-particles. This is because of the weak interactions. If the particles decaying into new particles result in some missing energy, one can also assume

dark matter relics to contribute in the new particles generated.

5.4 Non-thermal relics

Since WIMPs are not yet detected, and therefore disfavoured as dark matter particles, search for other thermal relics are useful. Non-thermal relics are particles which were not in thermal equilibrium in the plasma of the early Universe. If the relics are to be non-thermal the dark matter particles have to be produced at low temperatures so they never reach equilibrium in time, or they have to be decoupled from the primordial plasma. To be considered decoupled, they have to be very weakly interacting with the plasma [23].
Axion-like particles (ALPs), freeze-in models and decay products of primordial fields are three different classes of non-thermal relics.

Axion-like particles are produced non-thermally and their relic abundance are related to the details of the cosmological production mechanism. They are very light, and can relate to dark matter. Some ALPs can be WISP particles, weakly interacting Sub-eV particles. These particles may interact with ordinary matter through the exchange of very massive particles, and might decay into particles with very high energy scales [24].

The freeze-in scenarios cover the Feebly Interacting Dark Matter Particles (FIMPs). They are initially decoupled from the primordial thermal plasma because of their extremely weak coupling to the standard particles. This is considered to be opposite interactions to the freeze-out. These particles are mostly undetectable [25].

The particles that are massive and very weakly-interacting can also have been generated non-thermally in the early Universe. This happens by the decay of primordial fields during phase transitions. Even though the particles are to weakly coupled to Standard Model particles, other unstable new particles can also exist. They can thermalize, and decay into dark matter. The next-to-lightest new particle is in general stable over a long time because of its very weak coupling to the dark matter particles, before decaying into dark matter. Dark matter could have been gravitationally produced by Hawking evaporation of primordial black holes. [26].
Dark matter particles can be made of several new particles that originally can come from all of the relic scenarios.

6 Conclusion

In this thesis the existence of dark matter particles and their interaction with Standard Model particles has been looked at. The main goal was to look into the mechanism called freeze out and see if this is a good mechanism in the search for dark matter particles. The WIMPs were considered as the particles that interacted with the Standard Model particles in thermal freeze out. The interaction between the particles in thermal freeze out were compared to the Standard Model interactions, and it was found that weak interactions are quite similar.

When doing calculations to find the relic abundance and freeze out points for different particles DarkSUSY was used. In this program the annihilation cross section was fixed to a few different values and the results obtained for the relic abundance was compared to Planck's observed value of $\Omega_c h^2$ from 2018. The relic abundance obtained in DarkSUSY was also compared to the relic abundance found when using approximate solutions of the Boltzmann equation. From this it was found that the approximate solutions of the Boltzmann equation are quite good for calculating the relic abundance of cold dark matter in the Universe.

In the search for dark matter it has been looked at the evidence found in gravitational effects in the galaxies, galaxy clusters and some larger scaled structures as well. There has been found good evidence for dark matter. In addition to thermal relics produced from freeze out, there are also non thermal relics that interact differently. When it comes to detecting and actually observing the dark matter, there is still some more work that needs to be done. However, the cross sections used for the particles included in the WIMP miracle is most likely too big to be able to detect any dark matter. More thinking should be done about what kind of particles dark matter particles could be. They might not be as heavy as assumed in the WIMP miracle.

References

[1] A. Arbey and F. Mahmoudi, *Dark matter and the early Universe: a review*, Prog. Part. Nucl. Phys. **119** (2021), 103865 doi:10.1016/j.ppnp.2021.103865 [arXiv:2104.11488 [hep-ph]].

[2] V. A. Rubakov, *Cosmology and Dark Matter*, [arXiv:1912.04727 [hep-ph]].

[3] F. Melia, *The Friedmann–Lemaître–Robertson–Walker metric*, Mod. Phys. Lett. A **37**, no.03, 2250016 (2022) doi:10.1142/S021773232250016X

[4] T. Padmanabhan, *Cosmological constant: The Weight of the vacuum*, Phys. Rept. **380**, 235-320 (2003) doi:10.1016/S0370-1573(03)00120-0 [arXiv:hep-th/0212290 [hep-th]].

[5] E. W. Kolb and M. S. Turner, *The Early Universe*, Front. Phys. **69**, 1-547 (1990) doi:10.1201/9780429492860

[6] N. Aghanim *et al.* [Planck], *Planck 2018 results. VI. Cosmological parameters*, Astron. Astrophys. **641**, A6 (2020) [erratum: Astron. Astrophys. **652**, C4 (2021)] doi:10.1051/0004-6361/201833910 [arXiv:1807.06209 [astro-ph.CO]].

[7] S. R. Green and R. M. Wald, *How well is our universe described by an FLRW model?*, Class. Quant. Grav. **31**, 234003 (2014) doi:10.1088/0264-9381/31/23/234003 [arXiv:1407.8084 [gr-qc]].

[8] P.A. Tipler, and R.A. Llewellyn, *Particle Physics*, in Modern Physics, Sixth edition, New York, USA, W.H Freeman and Company, (2012)

[9] M. K. Gaillard, P. D. Grannis and F. J. Sciulli, *The Standard model of particle physics*, Rev. Mod. Phys. **71**, S96-S111 (1999) doi:10.1103/RevModPhys.71.S96 [arXiv:hep-ph/9812285 [hep-ph]].

[10] Cush, 17.09.2019, *Standard Model of Elementary Particles*, [Online] https : //no.m.wikipedia.org/wiki/Fil : Standard_Model_of_Elementary_Particles.svg, Copied 04.05.2022

[11] M. Aaboud *et al.* [ATLAS], *Observation of $H \to b\bar{b}$ decays and VH production with the ATLAS detector*, Phys. Lett. B **786**, 59-86 (2018) doi:10.1016/j.physletb.2018.09.013 [arXiv:1808.08238 [hep-ex]].

[12] J. A. Formaggio and G. P. Zeller, *From eV to EeV: Neutrino Cross Sections Across Energy Scales*, Rev. Mod. Phys. **84**, 1307-1341 (2012) doi:10.1103/RevModPhys.84.1307 [arXiv:1305.7513 [hep-ex]].

[13] CERN, *Supersymmetry*, home.cern from https://home.cern/science/physics/supersymmetry, (downloaded: 04.04.2022)

[14] T. Bringmann and J. Edsjö, *DarkSUSY 6.3: Freeze-in, out-of-equilibrium freeze-out, cosmic-ray upscattering and further new feature*, [arXiv:2203.07439 [hep-ph]].

[15] T. Bringmann, J. Edsjö, P. Gondolo, P. Ullio and L. Bergström, *DarkSUSY 6 : An Advanced Tool to Compute Dark Matter Properties Numerically*, JCAP **07**, 033 (2018) doi:10.1088/1475-7516/2018/07/033 [arXiv:1802.03399 [hep-ph]].

[16] G. Bertone, D. Hooper and J. Silk, *Particle dark matter: Evidence, candidates and constraints*, Phys. Rept. **405**, 279-390 (2005) doi:10.1016/j.physrep.2004.08.031 [arXiv:hep-ph/0404175 [hep-ph]].

[17] E. Ardi and H. Baumgardt, *Depletion of dark matter within globular clusters*, J. Phys. Conf. Ser. **1503**, no.1, 012023 (2020) doi:10.1088/1742-6596/1503/1/012023

[18] D. Clowe, M. Bradac, A. H. Gonzalez, M. Markevitch, S. W. Randall, C. Jones and D. Zaritsky, *A direct empirical proof of the existence of dark matter*, Astrophys. J. Lett. **648**, L109-L113 (2006) doi:10.1086/508162 [arXiv:astro-ph/0608407 [astro-ph]].

[19] S. Dodelson, *Modern Cosmology*, Academic Press, Amsterdam, 2003

[20] M. D'Anna, G. Job, *An alternative approach to the Boltzmann distribution through the chemical potential*, 38, 2014, doi:10.1393/ncc/i2015-15090-5

[21] L. Husdal, *On Effective Degrees of Freedom in the Early Universe*, Galaxies **4**, no.4, 78 (2016) doi:10.3390/galaxies4040078 [arXiv:1609.04979 [astro-ph.CO]].

[22] 01.08.2006, *Feynman EP Annihilation.png*, /Online]https : //commons.wikimedia.org/wiki/File : Feynman_EP_Annihilation.png, Copied 04.05.2022

[23] H. Baer, K. Y. Choi, J. E. Kim and L. Roszkowski, *Dark matter production in the early Universe: beyond the thermal WIMP paradigm*, Phys. Rept. **555**, 1-60 (2015) doi:10.1016/j.physrep.2014.10.002 [arXiv:1407.0017 [hep-ph]].

[24] K. Ehret [ALPS], *The ALPS Light Shining Through a Wall Experiment - WISP Search in the Laboratory*, [arXiv:1006.5741 [hep-ex]].

[25] S. Bhattacharya, S. Chakraborti and D. Pradhan, *Electroweak Symmetry Breaking and WIMP-FIMP Dark Matter*, [arXiv:2110.06985 [hep-ph]].

[26] N. Bernal and Ó. Zapata, *Dark Matter in the Time of Primordial Black Holes*, JCAP **03**, 015 (2021) doi:10.1088/1475-7516/2021/03/015 [arXiv:2011.12306 [astro-ph.CO]].